

## Molecular-dynamics investigation of tracer diffusion in a simple liquid: Test of the Stokes-Einstein law

F. Ould-Kaddour\* and D. Levesque

*Laboratoire de Physique Théorique, Université de Paris–Sud, 91405 Orsay Cédex, France<sup>†</sup>*

(Received 7 February 2000; published 21 December 2000)

In this work, we study the diffusion of solute particles in the limit of infinite dilution in a solvent. An estimate is made of the solute concentration below which this limit is attained. We determine the range of the size and mass values of the solute particles where the solute diffusion coefficient is well estimated from the Stokes-Einstein formula. For these aims, extensive molecular-dynamics simulations are carried out for a model tracer-solvent system made up of 5324 molecules including solvent and tracer molecules interacting through Lennard-Jones potentials. The values of the viscosity coefficient, corrected for long time tail contributions, and the diffusion coefficients are obtained with high precision. Positive deviations from the Stokes-Einstein formula are observed as the size ratio or the mass ratio of the tracer to solvent molecules is lowered. For equal solvent and tracer molecular masses, the crossover to the hydrodynamics regime is found to occur when the size ratio is  $\sim 4$ . The results show a strong coupling between the size and mass effects on the tracer diffusivity, with the latter being predominant. An analysis of the molecular-dynamics data in the hydrodynamic regime shows that the Stokes-Einstein formula holds for this system with *slip* boundary conditions and the hydrodynamic radius equal to the cross radius between the tracer-solvent molecules. The friction coefficient is evaluated from the computed autocorrelation function of the force exerted by the fluid on the tracer molecule, following a scheme proposed by Lagar'kov and Sergeev; it is found that the latter criterion gives the correct diffusion coefficient only in the limits of high sizes and high masses.

DOI: 10.1103/PhysRevE.63.011205

PACS number(s): 66.20.+d, 02.70.Ns, 05.40.Jc

### I. INTRODUCTION

Understanding diffusion and measuring diffusion constants of molecules in liquids are fundamental problems in statistical mechanics and the physics of the liquid state. They are important for basic and applied problems in physical chemistry and biology since many processes are diffusion limited. Most of the mixtures and solutions of these two domains are characterized by very large size and mass ratios between the solute and solvent molecules. It is well established that the diffusion coefficient  $D$  for a large and massive solute molecule of radius  $\sigma$  in a solvent of much smaller and lighter molecules is related to the solvent viscosity  $\eta$  by the Stokes-Einstein (SE) formula

$$D = \frac{k_B T}{f \pi \eta \sigma}, \quad (1)$$

where  $T$  is the absolute temperature,  $k_B$  the Boltzmann constant, and  $f$  a numerical constant determined by the choice of *stick* or *slip* hydro-dynamic boundary conditions at the solute surface. This relation has been verified experimentally in great detail [1] and is theoretically well understood through Brownian particle dynamics [2]. If, however, the solute size and mass are comparable to those of the solvent molecules then Eq. (1) is not expected to be valid, and a microscopic approach becomes necessary. Such investigations have been made possible only due to computer simulations and theoret-

ical studies in which solute size and mass can be varied independently of each other. Alder, Alley, and Dymond [3] investigated the mass and size dependence of the diffusion constant in moderately dense hard-sphere mixtures in order to study the deviations from Enskog theory due to the appearance of correlated motions in the fluid. An investigation of diffusion in binary Lennard-Jones mixtures has also been reported [4].

However, for tracer diffusion, i.e., diffusion of one component at infinite dilution in a solvent, the existing data are very limited [5]. One of us [6] has investigated small tracer diffusion in a dense Lennard-Jones (LJ) fluid by using molecular-dynamics (MD) simulations but the calculations were performed for a rather small system of 108 molecules and a concentration of tracer molecules of 12%, which would be considered more as a binary system than as a solution at infinite dilution. Recently, Bocquet, Hansen, and Piasecki [7] have calculated the friction coefficient exerted by a hard-sphere fluid on an infinitely massive Brownian sphere as a function of the size ratio between the Brownian particle and the fluid spheres, both analytically using microscopic kinetic theory and with molecular-dynamics simulations. They found that the SE formula holds with stick boundary conditions in the range of size ratio between 1 and 4.5. The apparent validity of stick boundary conditions is rather surprising since the slip boundary condition is more expected for a system of elastic hard spheres, which has no attractive intermolecular interactions. Brey and Ordóñez [8] have studied, by MD simulations, a system of particles interacting through a LJ potential containing a heavy test particle. They have attempted to evaluate the friction coefficient of the test particle from a Green-Kubo formula by using an appropriate cutoff in the time integration of the autocorrela-

\*Permanent address: Institut de Physique, Université de Tlemcen, BP119, Tlemcen 13000, Algérie.

<sup>†</sup>Unité Mixte de Recherche, Université Paris–Sud, CNRS 8627.

tion function of the force acting on this particle. Their analysis of the validity of the SE formula is less conclusive since the viscosity value of the solvent is computed only within an error of 20%.

From an experimental point of view, it is clearly difficult to find a set of mixtures that allows a systematic study of the dependence of the diffusion coefficient on the mass and size ratio without affecting the intermolecular interactions. Such an experimental study has been reported for the diffusion of xenon in *n*-alkanes [9], which has led to the conclusion that in order to maintain a simple relation between the xenon diffusion coefficient and the solvent viscosity  $\eta$  the experimental data should be fitted empirically by a modified SE formula by adding an exponent to the viscosity coefficient appearing in Eq. (1). More recently, the diffusion coefficients of the molecule  $C_{60}$  in toluene, benzene, and carbon tetrachloride at 303.15 K have been reported by Castillo, Garza, and Ramos [10]. The value of the viscosity coefficient has also been measured, which has allowed a direct estimation of the value of the hydrodynamic diameter of the  $C_{60}$  molecule from the SE formula [Eq. (1)]. This latter is compared to the value extracted from x-ray studies. It is found that for the stick boundary condition the hydrodynamic diameter of  $C_{60}$ /toluene,  $C_{60}$ /benzene, and  $C_{60}/CCl_4$  has, respectively, a value that deviates from the crystallographic value by 22.8%, -53.5%, and -7.7%, and for the slip boundary condition the deviation is, respectively, 84.2%, -30.1%, and 38.87%. It is important to note that benzene, toluene, and  $CCl_4$  have mainly van der Waals type of interaction. Therefore these systems would be similar to some of those investigated in the present work.

In order to overcome the limitations, already mentioned above, of the work reported in Ref. [6], which uses a relatively small system, we have undertaken in the present paper extensive MD simulations for a tracer-solvent system made of 5324 molecules including solvent and tracer molecules. All the molecules interact through pair LJ potentials. In order to test the validity of the SE formula the value of the shear viscosity of the solvent is required. This latter is obtained by the appropriate Green-Kubo formula, taking carefully into account the corrections due to the long time tail that exists in the time-stress autocorrelation functions. The knowledge of the viscosity coefficient with a high precision has allowed us to investigate the SE formula unambiguously, by assessing the influence of the size and mass ratios on the tracer diffusivity separately. We have investigated a range of size ratio between 0.1 and 4, and a range of mass ratio between 0.1 and 120.

We have concentrated all along on the accurate appraisal of the statistical uncertainty of the results, and therefore obtain a good location of the crossover to the hydrodynamic regime. For example, this crossover is located for equal masses between solvent and solute molecules at a size ratio larger than 4. It occurs, for a fixed size ratio of 0.5, at a mass ratio more than 40. We also compute the autocorrelation function of the force acting on a tracer molecule in the regime of high mass and size ratio; this latter is used to compute the friction coefficient. The tracer diffusion coefficient

as calculated from the friction coefficient is compared to that obtained from the mean square displacement.

The paper is organized as follows. Section II describes our model and numerical procedures. The result for the shear viscosity of the solvent is presented in Sec. III. In Sec. IV, the value of the solute concentration is determined for which the infinite dilution is reached. In Sec. V, we present the results on the size and mass dependence of the tracer diffusion coefficient, together with an analysis of the SE formula in the high mass and/or the high size ratio regime. The calculation of the diffusion coefficient from the friction coefficient is discussed in Sec. VI. The paper ends with a discussion.

## II. MODEL AND NUMERICAL PROCEDURE

The system consists of a number  $N$  of molecules equal to 5324 including the tracer molecules. The index 1 refers to the solvent and 2 to the tracer. The pair intermolecular potentials are taken to be LJ potentials, modified with a cubic spline [11]:

$$U_{ij}(r) = \epsilon_{ij} f\left(\frac{r}{\sigma_{ij}}\right), \quad (2)$$

with additive diameters  $\sigma_{ij} = (\sigma_i + \sigma_j)/2$ . The function  $f(x)$  reads

$$f(x) = \begin{cases} 4(x^{-12} - x^{-6}) & \text{for } x < x_c \\ \frac{6}{610009} \left(67 - 48 \frac{x}{x_c}\right)^2 & \text{for } x_c < x < x_m \\ 0 & \text{for } x > x_m, \end{cases} \quad (3)$$

where  $x_c = (26/7)^{1/6}$  is the inflection point of the LJ potential and  $x_m = 67x_c/48$ . The units of energy, length, and mass were chosen to be, respectively,  $\epsilon_{11}$ ,  $\sigma_1$ , and  $m_1$ . All molecules have the same coupling constant  $\epsilon_{12} = \epsilon_{22} = \epsilon_{11}$ . The corresponding microscopic time scale is  $\tau = (m_1 \sigma_1^2 / \epsilon_{11})^{1/2}$ . Therefore the state of our system is specified through the overall reduced number density and temperature  $\rho^* = \rho \sigma_1^3$  and  $T^* = k_B T / \epsilon_{11}$ , the number concentration of tracer molecules  $N_2/N$ , and the values of the size ratio  $\sigma_2/\sigma_1$  and mass ratio  $m_2/m_1$ . The values for the density and temperature for the present calculations are  $\rho^* = 0.85$  and  $T^* = 1.0$ , specifying a dense liquid state near the triple point of the LJ system.

The simulations were carried out at constant volume and temperature using the standard Verlet algorithm and Hoover's thermostating method [12], with the time step  $\Delta t = 0.005\tau$ . Typical simulation runs are carried out for 10 000 to 20 000 equilibration time steps followed by 80 000 to 160 000 time steps during which the different time dependent correlation functions are computed. The diffusion coefficients  $D_1$  and  $D_2$  of the solvent and tracer molecules are obtained from the mean square displacement of the solvent and tracer molecules given by

$$D_i = \lim_{t \rightarrow \infty} \frac{1}{6tN_i} \sum_{j=1, N_i} \langle |\mathbf{r}_j^i(t) - \mathbf{r}_j^i(0)|^2 \rangle, \quad i=1,2, \quad (4)$$

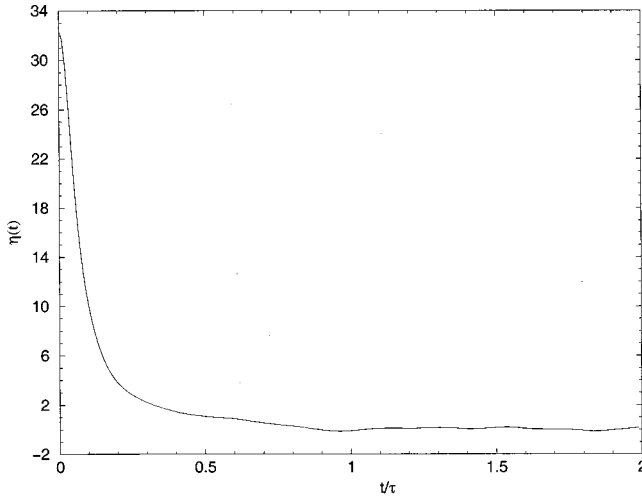


FIG. 1. Solvent shear viscosity autocorrelation function  $\eta(t)$  as a function of time  $t$  relative to the time scale  $\tau$ . The reduced density is  $\rho^* = 0.85$  and the reduced temperature is  $T^* = 1$ .

where  $\mathbf{r}_j^i(t)$  are the positions of the particles at time  $t$ . The shear viscosity coefficient for the pure solvent ( $N_2 = 0$ ) is obtained through the Green-Kubo formula

$$\eta = \int_0^\infty \eta(t) dt \quad (5)$$

with the shear viscosity autocorrelation function

$$\eta(t) = \frac{\rho_s}{3k_B T} \sum \frac{\langle \tau^{xy}(0) \tau^{xy}(t) \rangle}{N}. \quad (6)$$

Here the sum is to be made on the circular permutation of the indices  $xy$ ,  $\rho_s$  is the solvent density, and  $\tau^{xy}$ , the component of the microscopic stress tensor, is given by

$$\tau^{xy}(t) = \sum_{i=1}^N \left( m_i v_i^x v_i^y - \frac{1}{2} \sum_{i \neq j} \frac{r_{ij}^x r_{ij}^y}{r_{ij}} \frac{\partial U_{ij}}{\partial r_{ij}} \right), \quad (7)$$

where  $\mathbf{v}_i$  are the solvent particle velocities. We also compute the velocity autocorrelation function, and the different thermodynamic quantities and pair correlation functions.

### III. SHEAR VISCOSITY OF THE SOLVENT

The shear viscosity autocorrelation function  $\eta(t)$  of the solvent as a function of time  $t$  relative to the time scale  $\tau$  is given in Fig. 1. The final time  $t_f$  reached is equal to 2, significantly longer than those reported in previous simulations [13,14]. The total number of integration steps is equal to 260 000. The evaluation of the statistical error involved in the calculation of the viscosity is made by dividing the total simulation into intervals of 20 000 integration steps, for which the viscosity coefficient is calculated. From these values, a mean square deviation is evaluated, and from the mean square deviation we obtain the estimated statistical error for the entire simulation. The value of the viscosity coefficient found is

$$\eta = 3.56 \pm 0.04. \quad (8)$$

This amount of 1.2% in the statistical error is much lower than that reported in the literature [13–15]. This could be due to the long time equilibration of the different starting configurations and to the use of a statistical ensemble different from that in previous work, the Hoover thermostating method, which suppresses thermal fluctuations.

It is well known that the time correlation functions for fluid transport coefficients decay algebraically at long times. The long time tail behavior for the viscosity autocorrelation function of a dense fluid has been discussed in great detail in the literature [16,17]. One first correction to this asymptotic time behavior has been predicted by mode-coupling theory and is of an exponential form. The expressions for the asymptotic behavior and for this correction have been given in terms of the values of the transport coefficients [17]. The first one is of the form  $t^{-3/2}$  and reads for the viscosity autocorrelation function,

$$\lim_{t \rightarrow \infty} \eta(t) \sim \alpha t^{-3/2}, \quad (9)$$

with

$$\alpha = \frac{1}{120 \pi^{3/2} \beta^2} \left( \frac{7}{(2\nu)^{3/2}} + \frac{1}{\Gamma_s^{3/2}} \right), \quad (10)$$

where  $\nu = \eta / \rho_s m_1$ ,  $\beta = 1/k_B T$ , and

$$\Gamma_s = \frac{(\gamma - 1)\lambda}{\rho_s C_p} + \frac{4\nu}{3} + \frac{\zeta}{\rho_s m_1}, \quad (11)$$

in which  $\lambda$  is the thermal conductivity,  $\zeta$  is the bulk viscosity, and  $\gamma = C_p / C_v$  with  $C_p$  and  $C_v$  the specific heat capacities at constant pressure and volume, respectively. The exponential correction given by the extended mode-coupling theory of Kirkpatrick [18], van Beijeren [19], and de Scheper, Haffmans, and van Beijeren [20] has a simple form for a hard-sphere system. As the system we consider here is a highly dense fluid where hard-core effects are dominant, we shall follow the suggestion made by Erpenbeck [14] to use the simple form of a hard-sphere system to analyze our long time data. The extended mode-coupling contribution reads for a hard-sphere system of diameter  $\sigma_s$  [20]

$$\eta_{MC}(t) = (2 \eta_E / t_\sigma) A(\rho) \exp[-2Z_h(K_G)t], \quad (12)$$

in which  $\eta_E$  is the Enskog value of the viscosity,  $t_\sigma = (\beta m_1)^{1/2} \sigma_s / 2$ ,  $A$  is an amplitude known in terms of the structure factor, and  $Z_h(K_G)$  is the extended hydrodynamic mode eigenvalue for the heat mode evaluated at the ‘‘de Gennes minimum,’’ given approximately as a function of density by

$$Z_h(K_G) = 4.18(1.056 - \rho_s) / t_\sigma. \quad (13)$$

To estimate the order of magnitude of the coefficient  $\alpha$  in Eq. (9), which gives the amplitude of the long time tail, we use the values for the transport coefficients and heat capacities given in Ref. [13]. The resulting value is found to be

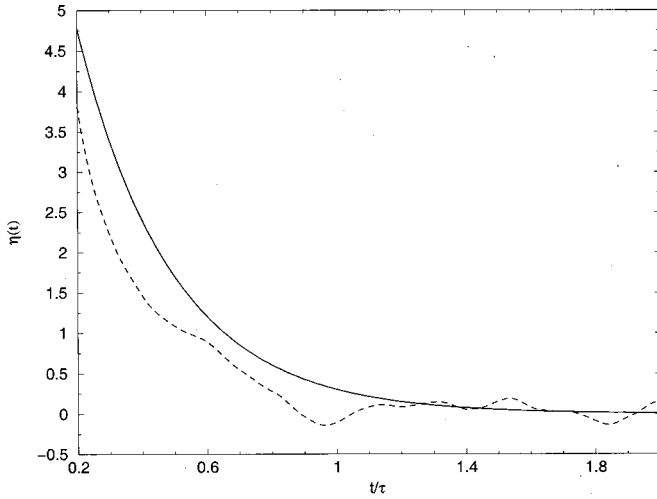


FIG. 2. Long time data of the solvent shear autocorrelation function as given in Fig. 1. The full curve is the fitted autocorrelation function as computed by the extended mode-coupling theory.

equal to  $4.9 \times 10^{-4}$ . For the largest time  $t_f$  where  $\eta(t)$  is evaluated, the correction from the long time tail to the viscosity coefficient is given by

$$\delta\eta = \frac{2\alpha}{\sqrt{t_f}}. \quad (14)$$

For our simulations  $\delta\eta \approx 7 \times 10^{-4}$ . This contribution to the viscosity is negligible at the present level of statistical accuracy.

By contrast, the contribution of the exponential term is significant. We use the LJ parameter  $\sigma_1$  for the hard-sphere diameter  $\sigma_s$  in  $t_\sigma$  and make a least squares fit to the data at long time from time 0.8 to  $t_f$ , in order to get the amplitude. The result is  $\eta_{MC} = 9.521 \exp(-3.444t/\tau)$ . Figure 2 shows the long time data of the shear viscosity autocorrelation function together with the fitted theoretical curve. We can see that the fitted exponential decay joins the MD data smoothly within statistical error at time  $t = 1.6\tau$ . The resulting increment to the viscosity coefficient is

$$\delta\eta_{MC} = \int_{t_f}^{\infty} \eta_{MC}(t) dt = 0.0028, \quad (15)$$

yielding the final estimate for the viscosity coefficient as

$$\eta = 3.57 \pm 0.04, \quad (16)$$

if we estimate the uncertainty on the correction  $\delta\eta_{MC}$  to be around 30%. The coupling between the modes associated with the shear waves and sound waves traversing the simulation box should affect the decay of  $\eta(t)$  only for times larger than  $t_c \sim L/c = 3.6 > t_f$  since  $L$ , the side of the simulation box, is  $18.4\sigma_1$  and the sound velocity  $c$  is estimated to be around 5 in reduced units [13].

TABLE I. Thermodynamic state properties and diffusion coefficients for the LJ system as a function of the number of tracer molecules. The reduced density  $\rho^* = 0.85$  and the reduced temperature  $T^* = 1.0$ . The size ratio  $\sigma_2/\sigma_1 = 0.5$  and mass ratio  $m_2/m_1 = 1.0$ .  $N_2$  is the number of tracer molecules.  $n_{\text{steps}}$  is the total number of time steps.  $U_i/\epsilon_{11}$  is the internal energy of the system,  $P/\rho k_B T$  is the compressibility factor,  $C_v$  is the specific heat at constant volume, and  $D_1$  and  $D_2$  are the diffusion coefficients of the solvent and solute molecules, respectively.

| $N_2$ | $n_{\text{steps}}$ | $U_i/\epsilon_{11}$ | $P^*/\rho^*T^*$ | $C_v$  | $D_1$       | $D_2$    |
|-------|--------------------|---------------------|-----------------|--------|-------------|----------|
| 3     | 220 000            | -2.6067             | 4.2062          | 2.5703 | 0.047 05(6) | 0.118(3) |
| 6     | 160 000            | -2.6138             | 4.1785          | 2.6036 | 0.047 00(6) | 0.113(2) |
| 12    | 160 000            | -2.6149             | 4.1500          | 2.5899 | 0.047 03(7) | 0.114(1) |
| 24    | 100 000            | -2.6081             | 4.0987          | 2.5805 | 0.047 39(8) | 0.119(1) |
| 48    | 60 000             | -2.5925             | 4.0021          | 2.5677 | 0.048 1(1)  | 0.120(1) |
| 96    | 40 000             | -2.6236             | 4.3459          | 2.5696 | 0.050 4(2)  | 0.125(2) |

#### IV. INFINITE DILUTION LIMIT

In Table I, we give the solvent  $D_1$  and tracer  $D_2$  diffusion coefficients as a function of the number of tracer molecules for a size ratio of  $\sigma_2/\sigma_1 = 0.5$  and mass ratio  $m_2/m_1 = 1$ . For each computation, we give the number of time steps and the values of the internal energy, pressure, and specific heat at constant volume. The time autocorrelation functions of positions and velocities are evaluated over  $400\Delta t$ . From partial averages of these correlation functions performed every 2000 time steps, the statistical error at a given time is estimated by evaluating the mean standard deviation of these averages. A typical graph for the mean square displacement as a function of time is shown in Fig. 3. The diffusion coefficient is obtained from the slope at long time together with the statistical error on the slope. In order to reach the same level of statistical error on  $D_2$ , the number of integration time steps in the simulation runs is increased as the number of tracer molecules is lowered, as shown in Table I. The statistical error-

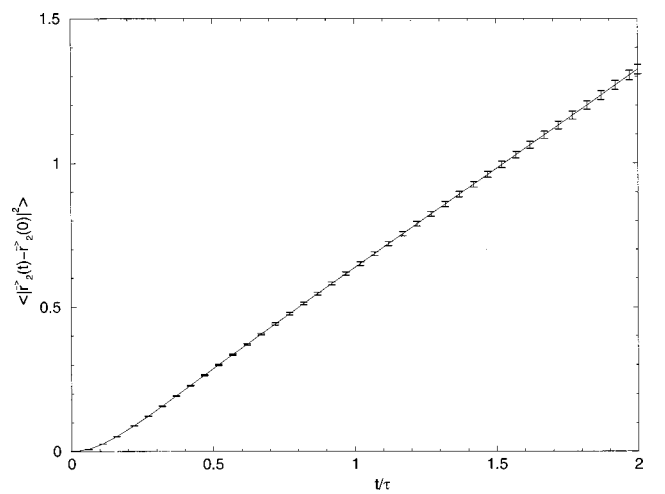


FIG. 3. Mean square displacement with error bars of the tracer molecule as a function of time  $t$  relative to the time scale  $\tau$ . The ratios  $\sigma_2/\sigma_1 = 0.5$  and  $m_2/m_1 = 1.0$ .

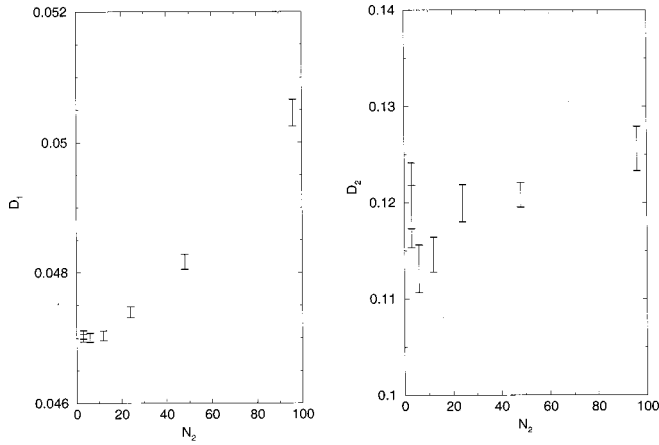


FIG. 4. Solvent and solute diffusion coefficient  $D_1$  and  $D_2$  as functions of the number of solute molecules.

obtained in the computation of the tracer diffusion coefficient is about 1.2%, and that on the solvent diffusion coefficient is 0.1%.

Figure 4 shows the tracer and solvent diffusion coefficients as a function of number of tracer molecules  $N_2$  for a size ratio of 0.5 and a mass ratio of 1. We can see that the solvent diffusion coefficient goes to a constant value, within the statistical error, below a number of tracer molecules equal to 20. Similar behavior is given for  $D_2$  within the statistical error. We can state, from both figures, that the infinite dilution limit is reached below a concentration of 0.3%, which is rather low for even such a noncharged system. A similar analysis performed for other size ratios considered in this work showed that the infinite dilution limit is obtained for a decreasing value of  $N_2$  as the size ratio increases. Therefore, we consider in the following studies the number of tracer molecules  $N_2=1, 2, 3, 6,$  and  $12$  for size ratio respectively 4.0, 3.0, 2.0, 1.5, and 0.5.

TABLE II. Solvent and tracer diffusion coefficients  $D_1$  and  $D_2$  as a function of the size ratio  $\sigma_2/\sigma_1$ . The mass ratio  $m_2/m_1=1.0$ .  $N_2$  is the the number of tracer molecules considered in each case and  $\rho^*$  is the reduced density. We also include the tracer diffusion coefficient as given by the SE formula for the slip and stick boundary conditions.

| $\sigma_2/\sigma_1$ | $N_2$ | $\rho^*$ | $D_1$       | $D_2$       | $D_{2\text{slip}}$<br>(SE) | $D_{2\text{stick}}$<br>(SE) |
|---------------------|-------|----------|-------------|-------------|----------------------------|-----------------------------|
| 0.1                 | 12    | 0.85     | 0.047 20(9) | 0.436(8)    | 0.040                      | 0.026                       |
| 0.3                 | 12    | 0.85     | 0.047 10(8) | 0.206(3)    | 0.034                      | 0.022                       |
| 0.5                 | 12    | 0.85     | 0.047 03(7) | 0.114(1)    | 0.029                      | 0.019                       |
| 0.7                 | 12    | 0.85     | 0.047 05(8) | 0.077(1)    | 0.026                      | 0.017                       |
| 1.0                 | solv  | 0.85     | 0.047 05(8) | 0.047 05(8) | 0.022                      | 0.014                       |
| 1.5                 | 6     | 0.848    | 0.046 72(8) | 0.028 3(8)  | 0.017                      | 0.017                       |
| 2.0                 | 6     | 0.845    | 0.046 58(9) | 0.018 6(4)  | 0.014                      | 0.01                        |
| 3.0                 | 2     | 0.84     | 0.047 28(7) | 0.11 8(3)   | 0.011                      | 0.007                       |
| 4.0                 | 1     | 0.84     | 0.048 3(1)  | 0.008 4(4)  | 0.0088                     | 0.0058                      |

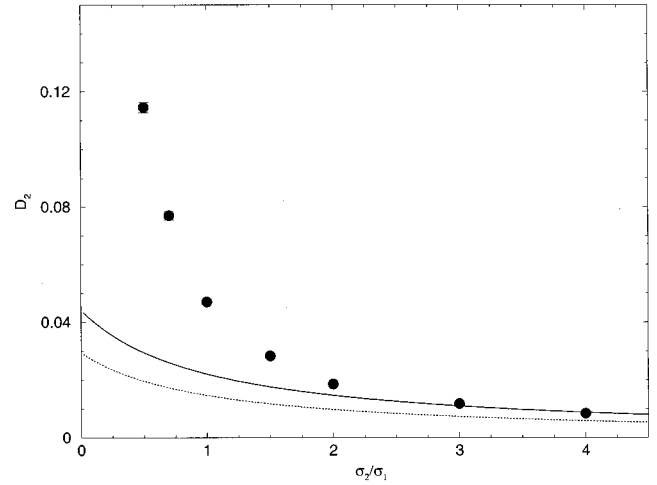


FIG. 5. Solute diffusion coefficient  $D_2$  as a function of the size ratio  $\sigma_2/\sigma_1$ . The mass ratio  $m_2/m_1=1.0$ . Full dots MD data; full curve, SE formula with slip boundary condition; dotted curve, SE formula with stick boundary condition. Statistical errors on MD data are smaller than symbol size.

## V. SIZE AND MASS DEPENDENCE

### A. Size dependence

The results for the size dependence of the tracer diffusion are given in Table II and Fig. 5, for the case of mass ratio equal to 1. For size ratios higher than 1, the pressure value of the system increases, and, in order to maintain a constant value of this latter, the volume of the box was slightly increased by an amount that corresponds to the excess volume occupied by the big tracer molecule with respect to the volume occupied by a solvent molecule (cf. the density values in Table II).

It is the main interest of the present work to investigate the SE formula given by Eq. (1), which we write again for  $D_2$  as

$$D_2 = \frac{T^*}{f\pi\eta^*\sigma_{12}^*}, \quad (17)$$

where the constant  $f=4$  and  $6$  for the the slip and stick hydrodynamic boundary conditions, respectively, and  $\sigma_{12}^*$  is the cross radius of the solvent-tracer molecules,  $\sigma_{12}^*=0.5(\sigma_2+\sigma_1)/\sigma_1$ . The choice of the cross radius  $\sigma_{12}^*$  is justified below. We plot in Fig. 5 the diffusion coefficient as given by the SE formula with the value of the solvent viscosity given in Eq. (16). The SE formula is found to approach the MD data with the slip (full curve) boundary conditions when the size ratio approach the value of 3. Below this size the SE relation strongly underestimates the diffusion coefficient of the tracer. For example, the ratio of the diffusion coefficient as obtained from the MD data to that given by the SE relation is

$$D_{2(\text{MD})}/D_{2(\text{SE})}=4 \quad \text{for } \sigma_2/\sigma_1=0.5. \quad (18)$$

The slip boundary condition seems in the present work to hold better than the stick boundary condition, which is more expected for a LJ type of interaction between solute and solvent molecules.

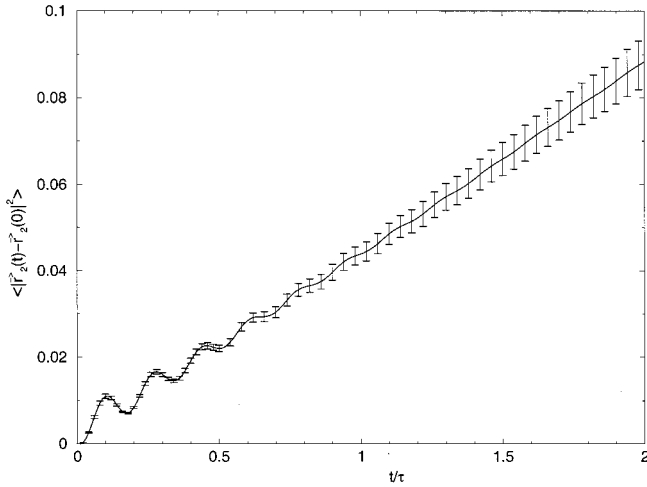


FIG. 6. Mean square displacement of the tracer molecule as a function of time  $t$  relative to the time scale  $\tau$ . The ratios  $\sigma_2/\sigma_1 = 4.0$  and  $m_2/m_1 = 1.0$ .

There is a change in the type of motion of the big tracer molecules as illustrated by the mean square displacement as a function of time plotted in Fig. 6 for  $\sigma_2/\sigma_1 = 4$  as compared to that shown in Fig. 3 for  $\sigma_2/\sigma_1 = 0.5$ . We can see that a big tracer molecule experiences many backscattering effects, which indicates that its motion stays correlated on a relatively long time scale of the order of 1, and is not of a Brownian type over this interval of time.

### B. Mass dependence

The dependence of  $D_2$  on the mass ratio  $m_2/m_1$  has been investigated for several size ratios of 0.5, 1.5, 3, and 4. The results are given in Tables III and IV. Figure 7 shows the mass dependence for a size ratio of 0.5. We can see that the hydrodynamical limit, i.e., mass independent behavior, is

TABLE III. Tracer diffusion coefficient as a function of the mass ratio  $m_2/m_1$  for a fixed size ratio  $\sigma_2/\sigma_1$ .

| $\sigma_2/\sigma_1 = 0.5$ |           | $\sigma_2/\sigma_1 = 1.5$ |           |
|---------------------------|-----------|---------------------------|-----------|
| $m_2/m_1$                 | $D_2$     | $m_2/m_1$                 | $D_2$     |
| 0.1                       | 0.179(3)  | 0.1                       | 0.0292(8) |
| 0.2                       | 0.158(3)  | 0.5                       | 0.0283(8) |
| 0.5                       | 0.137(2)  | 1                         | 0.0283(8) |
| 1                         | 0.114(1)  | 2                         | 0.0273(7) |
| 2                         | 0.103(1)  | 4                         | 0.0271(7) |
| 3                         | 0.098(2)  | 8                         | 0.0258(7) |
| 6                         | 0.087(1)  | 20                        | 0.0253(6) |
| 12                        | 0.068(1)  | 40                        | 0.0242(8) |
| 15                        | 0.063(1)  | 80                        | 0.0205(5) |
| 30                        | 0.041(1)  | 120                       | 0.0180(6) |
| 40                        | 0.0338(8) |                           |           |
| 60                        | 0.0336(7) |                           |           |
| 90                        | 0.0264(7) |                           |           |
| 120                       | 0.0251(5) |                           |           |

TABLE IV. Tracer diffusion coefficients  $D_2$  computed from the mean square displacement and  $D_2(\text{frict})$  computed from the friction coefficient, as a function of size and mass ratios.  $\Delta$  is the relative discrepancy between the two coefficients.

| $\sigma_2/\sigma_1$ | $m_2/m_1$ | $D_2$     | $D_2(\text{frict})$ | $\Delta(\%)$ |
|---------------------|-----------|-----------|---------------------|--------------|
| 4.0                 | 5         | 0.0075(4) | 0.0154              | 106          |
|                     | 10        | 0.0075(8) | 0.0122              | 61.6         |
|                     | 20        | 0.0075(5) | 0.0101              | 35.1         |
|                     | 40        | 0.0067(4) | 0.0092              | 37.0         |
|                     | 60        | 0.0077(5) | 0.0084              | 8.6          |
| 3.0                 | 40        | 0.0101(8) | 0.0135              | 33.6         |
|                     | 60        | 0.0097(7) | 0.0117              | 19.6         |
| 1.5                 | 4         | 0.0271(7) | 0.0448              | 65.3         |
|                     | 20        | 0.0253(6) | 0.034               | 34.38        |
|                     | 40        | 0.0242(8) | 0.0325              | 34.29        |
|                     | 80        | 0.0205(5) | 0.0276              | 34.6         |

reached for a mass above 40. Positive deviation from the SE formula appears as the value of the mass is decreased. From Tables III and IV, we note that as the tracer size is increased the hydrodynamic limit is reached for a lower mass. For example, for  $\sigma_2/\sigma_1 = 4$  the value of this mass shifts down to 5. Our simulations show that the effects of size and mass ratios between the solvent and solute molecules are strongly coupled.

A justification of the choice of the hydrodynamic radius  $\sigma_{12}^*$  is performed as follows. We consider the data lying in the hydrodynamic region of mass values for different sizes studied. In Fig. 8, a plot of  $D_2$  versus the inverse of  $\sigma_{12}^*$  shows a linear dependence. We define an effective radius as  $\lambda \sigma_{12}^*$  and determine  $\lambda$  from the SE formula written in the form

$$D_2 = \frac{1}{4\pi\eta^*\lambda\sigma_{12}^*}, \quad (19)$$

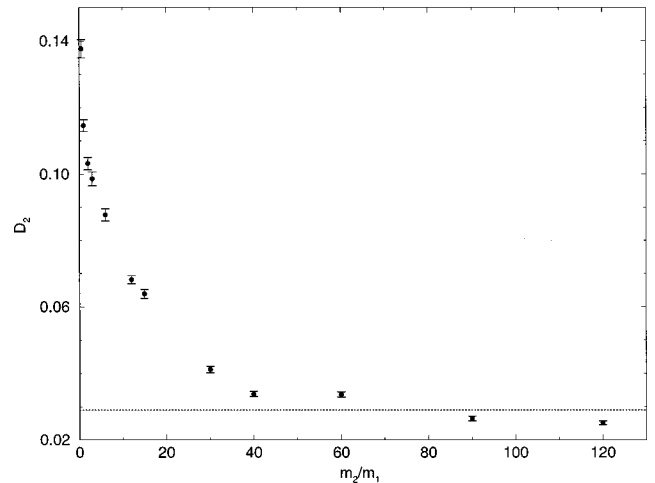


FIG. 7. Solute diffusion coefficient  $D_2$  as a function of the mass ratio  $m_2/m_1$ . The size ratio  $\sigma_2/\sigma_1 = 0.5$ . Dots with error bars, MD data; dotted line, value of  $D_2$  from SE formula with slip boundary condition.

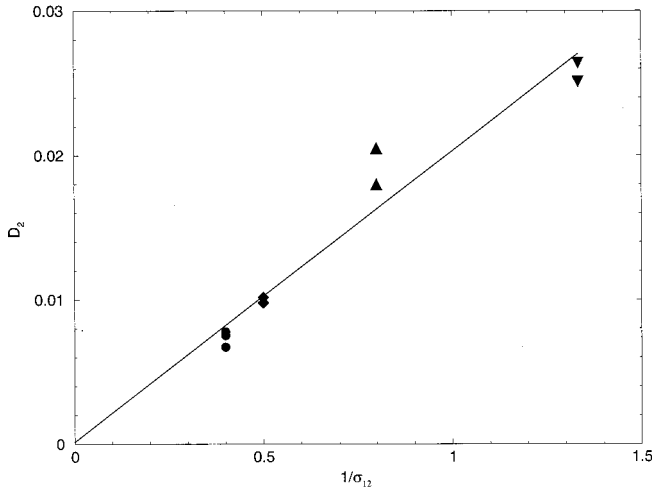


FIG. 8.  $D_2$  as a function of the inverse of the cross LJ parameter  $\sigma_{12}$ . Dots are for  $\sigma_2/\sigma_1=4$  and  $m_2/m_1=20,40,60$ . Filled diamonds are for  $\sigma_2/\sigma_1=3$  and  $m_2/m_1=40,60$ . Filled up triangles are for  $\sigma_2/\sigma_1=1.5$  and  $m_2/m_1=80,120$ . Filled down triangles are for  $\sigma_2/\sigma_1=0.5$  and  $m_2/m_1=90,120$ . Full line is linear fit to Eq. (19).

where use is made of the value for the viscosity we obtained, recalling that  $T^*=1.0$ . A linear fit gave a value for  $\lambda=1.1 \pm 0.1$ . This result justifies the use of a hydrodynamic radius of  $\sigma_{12}^*$ , which characterizes the range of repulsive interaction between solute and solvent molecules. This conclusion is in agreement with the result found by Bocquet and Barrat [21] that, at the contact between fluid and plane solid walls, the hydrodynamic boundary conditions on the velocity field applied at a surface separated from the solid by about one layer of fluid atoms. This value of  $\sigma_{12}$  represents also the radius of a channel in the solvent through which a solute molecule can drift away. Clearly, from our MD data, the use of the stick boundary condition would lead to a hydrodynamic radius of solute of  $4\sigma_{12}/6$ , a value that does not represent any characteristic length of the solute-solvent mixtures considered.

We plot in Fig. 9 the mean square displacement of a tracer molecule of a fixed size ratio of 1.5 and for mass ratios of 20 and 80. We can see that the increase in mass does not alter the tracer type of motion at short time except for being much slower. This illustrates once more the dominant effect of the size on the tracer diffusivity.

## VI. THE DIFFUSION AND FRICTION COEFFICIENTS

In the simple Langevin theory of Brownian dynamics the diffusion coefficient  $D$  of a Brownian particle is related to the friction coefficient  $\xi$  exerted by the fluid on the Brownian particle by the Einstein relation [22]

$$D = \frac{k_B T}{\xi}, \quad (20)$$

and a microscopic expression for the friction coefficient has been obtained through a Green-Kubo formula by Kirkwood [23] in the form

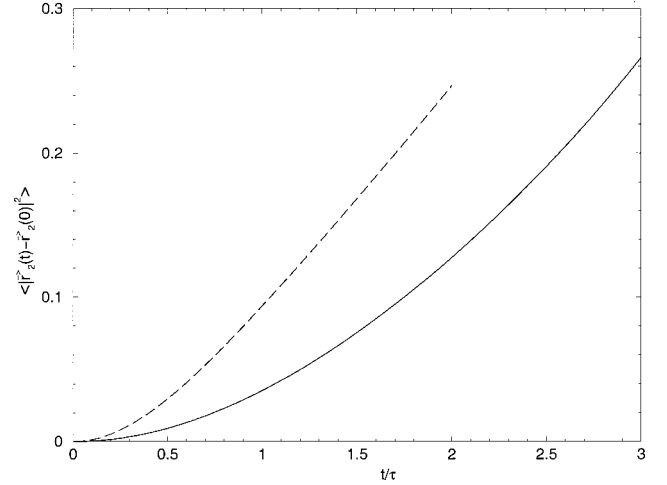


FIG. 9. Mean square displacement of the tracer molecule as a function of time  $t$  relative to the time scale  $\tau$ . Dashed curve, the ratios  $\sigma_2/\sigma_1=1.5$  and  $m_2/m_1=20$ ; full curve, the ratios  $\sigma_2/\sigma_1=1.5$  and  $m_2/m_1=80$ .

$$\xi = \frac{1}{3k_B T} \int_0^{\tau_0} \langle \vec{F}(t) \vec{F}(0) \rangle dt. \quad (21)$$

The expression in the integral is the autocorrelation function of the force exerted on the Brownian particle by the fluid. This expression for  $\xi$  vanishes if the upper bound in the integral is set to infinity [22]. The introduction of a cutoff time  $\tau_0$  was the solution to this problem given by Kirkwood, who assumed that the integral of the force autocorrelation function versus the upper bound presented a plateau region where it was almost independent of the precise value of  $\tau_0$ . The friction coefficient could then be evaluated from this plateau region. Lagar'kov and Sergeev [24] have proposed to choose as  $\tau_0$  the first zero of the force autocorrelation function.

As in Ref. [8], we propose to test the approach put forward by Lagar'kov and Sergeev by comparing the diffusion coefficients as obtained from Eqs. (20) and (21) with those determined from the mean square displacement [25]. The force exerted by the solvent on the tracer molecule is given directly by the MD simulations. To render the comparison significant, we consider data in the range of high size ratios and relatively high mass ratios.

In order to check the consistency of our computation of the force on the solute particle we have tested that  $\langle \vec{F}(0) \vec{F}(0) \rangle$  was equal, within statistical error, to the second time derivative of the tracer velocity autocorrelation function at time zero.

We give in Table IV the tracer diffusion coefficient  $D_2$  evaluated both from the mean square displacement and from the friction coefficient using the Lagar'kov and Sergeev criterion. The relative discrepancies between these two are shown in Table IV. It is found that the Lagar'kov and Sergeev criterion leads to an overestimation of the diffusion coefficient by about 30%. The best agreement, about 10%, is obtained only in the limit of both high size and mass ratio.

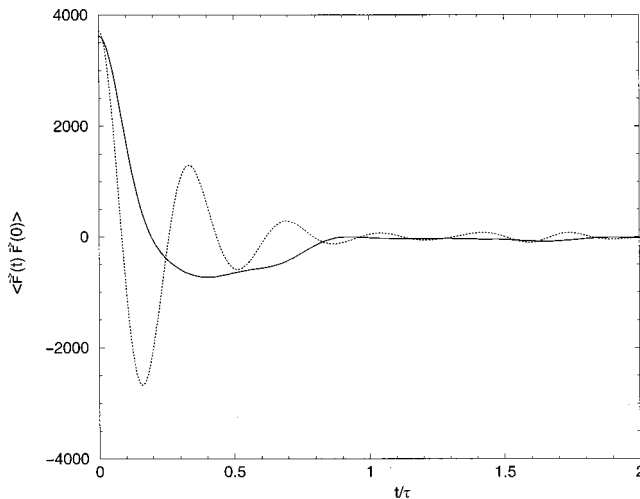


FIG. 10. Force autocorrelation function of solute particles as a function of time  $t$  relative to the time scale  $\tau$ . Full curve,  $\sigma_2/\sigma_1 = 4$  and  $m_2/m_1 = 60$ ; dotted curve,  $\sigma_2/\sigma_1 = 4$  and  $m_2/m_1 = 5$ .

These discrepancies, which can reach 100% for the case of a size ratio of 4 and a mass ratio of 5, are understood by looking at the decay behavior of the force autocorrelation function. In Fig. 10 we plot the force autocorrelation functions for a size ratio of 4 and mass ratios of 5 and 60. Clearly the force autocorrelation for the low mass case shows considerable temporal correlations, excluding the possibility of a plateau in the integral [Eq. (21)] if considered as a function of  $\tau_0$ . In the case of high mass we can see that the integral of the force autocorrelation function will be almost constant in the vicinity of a unique upper bound value corresponding to the first zero of  $\langle \vec{F}(t) \vec{F}(0) \rangle$ , and only in this case could the Lagar'kov and Sergeev criterion be used without ambiguity.

## VII. DISCUSSION

At the level of accuracy of the present MD data and system size, it seems that for a LJ system at constant pressure and temperature near the triple point, the tracer diffusion coefficients at high mass ratio and size ratio take values in agreement with the SE formula with a slip boundary condition between solute and solvent molecules, and with a hydrodynamic radius equal to the range of repulsive interaction between solute and solvent molecules. Our simulations show also that there is a strong coupling between the size and mass

effects on the tracer diffusivity, in the domains of size and mass ratio considered in this work. For stable suspensions of solute particles in the solvent, our results are compatible with a behavior of Brownian type as soon as the size ratio is higher than 3, for practically any mass ratio. Our results show that the use of Brownian dynamics for a size ratio of the order of unity is questionable as soon as the mass ratio is smaller than 10.

We stress that the high accuracy of the data for both the solvent viscosity and the diffusion coefficients has allowed a convincing investigation of the crossover toward the hydrodynamic behavior of solute particles and an evaluation of the shortcomings of the Lagar'kov and Sergeev proposal for the computation of the friction coefficient. Moreover, our results can partially explain the experimental data on the diffusion coefficient of  $C_{60}$  in toluene, benzene, and carbon tetrachloride solutions. Our finding that the hydrodynamic radius characterizes the range of interaction between solute and solvent molecules shows the strong dependence of this radius on the solute-solvent interaction. It is expected that due to the change in the type of interaction between  $C_{60}$  and the solvent molecules considered, the hydrodynamic radius should vary strongly from one solvent to another.

Finally, we quote the work reported by Bhattacharyya and Bagchi [26] on a microscopic and self-consistent calculation of the diffusion coefficient of a tagged particle in a dense LJ liquid. In this calculation the solute motion is coupled to both the collective density fluctuation and the transverse current mode of the liquid. They found that in dense liquids the relative importance of the hydrodynamic modes of the solvent in the motion of a solute particle is determined largely by the solute-solvent size ratio, and predicted that the crossover from the microscopic to the hydrodynamic regime should occur when the solute molecule is about 2–3 times larger than the solvent molecule for equal masses. These findings are in agreement with our results, and therefore we hope that the high accuracy of our MD data will allow a significant test of theoretical approaches to diffusion processes in dense fluids.

## ACKNOWLEDGMENTS

One of us (F.O.K.) acknowledges financial support from the International Center for Theoretical Physics, Trieste, Italy and La Société des Amis de la Science, Paris, France. The authors would like to thank the University of Tlemcen for supporting this research.

- 
- [1] G. Phillies, *J. Phys. Chem.* **85**, 2838 (1981).  
 [2] J.-P. Hansen and I. R. McDonald, *Theory of Simple Liquids* (Academic, London, 1986).  
 [3] B. J. Alder, W. E. Alley, and J. H. Dymond, *J. Chem. Phys.* **61**, 1415 (1974).  
 [4] R. J. Bearman and D. L. Jolly, *Mol. Phys.* **44**, 665 (1981).  
 [5] A. J. Eastale and L. A. Woolf, *Chem. Phys. Lett.* **167**, 329 (1990).  
 [6] F. Ould-Kaddour and J.-L. Barrat, *Phys. Rev. A* **45**, 2308 (1992).  
 [7] L. Bocquet, J.-P. Hansen, and J. Piasecki, *J. Stat. Phys.* **76**, 527 (1994).  
 [8] J. J. Brey and J. Gómez Ordóñez, *J. Chem. Phys.* **76**, 3260 (1982).  
 [9] G. L. Pollack and J. Enyeart, *Phys. Rev. A* **31**, 980 (1985).  
 [10] R. Castillo, C. Garza, and S. Ramos, *J. Phys. Chem.* **98**, 4188 (1994).  
 [11] B. L. Holian and D. J. Evans, *J. Chem. Phys.* **78**, 5147 (1983).

- [12] M. Allen and D. Tildesley, *Computer Simulation of Liquids* (Oxford University Press, Oxford, 1987).
- [13] D. Levesque and L. Verlet, *Mol. Phys.* **61**, 143 (1987).
- [14] J. J. Erpenbeck, *Phys. Rev. A* **38**, 6255 (1988).
- [15] M. Schoen and C. Hoheisel, *Mol. Phys.* **56**, 653 (1985).
- [16] J. R. Dorfman and E. G. D. Cohen, *Phys. Rev. A* **12**, 292 (1975).
- [17] M. H. Ernst, E. H. Hauge, and J. M. J. van Leeuwen, *J. Stat. Phys.* **15**, 23 (1976).
- [18] T. R. Kirkpatrick, *Phys. Rev. Lett.* **53**, 1735 (1984).
- [19] H. van Beijeren, *Phys. Lett.* **105A**, 191 (1984).
- [20] I. M. de Schepper, A. F. Haffmans, and H. van Beijeren, *Phys. Rev. Lett.* **57**, 1715 (1986).
- [21] L. Bocquet and J.-L. Barrat, *Phys. Rev. Lett.* **70**, 2726 (1993).
- [22] P. Résibois and M. De Leener, *Classical Kinetic Theory of Fluids* (Wiley, New York, 1977).
- [23] J. Kirkwood, *J. Chem. Phys.* **14**, 180 (1946).
- [24] A. N. Lagar'kov and V. H. Sergeev, *Usp. Fiz. Nauk* **125**, 409 (1978) [*Sov. Phys. Usp.* **21**, 566 (1978)].
- [25] P. Español and I. Zúñiga, *J. Chem. Phys.* **98**, 574 (1993).
- [26] S. Bhattacharyya and B. Bagchi, *J. Chem. Phys.* **106**, 1757 (1997).